Radiative and nonradiative decay rates of molecules adsorbed on clusters of small dielectric particles[a)]

Naomi Liver and Abraham Nitzan
Department of Chemistry, Tel Aviv University, Tel Aviv 69978, Israel

Karl F. Freed
Department of Chemistry and the James Franck Institute, University of Chicago, Chicago, Illinois 60637

(Received 17 July 1984; accepted 2 October 1984)

In this work we shall develop a formalism which extends previous calculations of lifetimes of excited molecular states near planar dielectric surfaces and near single small dielectric particles to situations where the molecule is adsorbed on a cluster made of several dielectric spherical grains. The nonradiative relaxation rate is seen to be relatively weakly dependent on the cluster structure and, if the molecule is adsorbed on one of the grains, is well approximated by the single grain result. The radiative decay rate and hence the quantum yield are much more sensitive to the geometry of the cluster which determines the position (in frequency) of the dielectric resonances of the cluster. The formalism developed here may be used to evaluate local field intensities at different positions within a cluster of dielectric grains under the influence of an external incident field.

I. INTRODUCTION

Following the discovery of surface enhanced Raman scattering[1] and the realization that much of the observed enhancement is due to the local electromagnetic field enhancement on rough metal surfaces and near metallics particles, it was pointed out that resonance optical phenomena such as fluorescence and photochemical processes involving adsorbed molecules should also be strongly affected.[2] Experimental evidence for such effects quickly accumulated.[3] Both theory and experiments indicate that the resonance optical response of molecules adsorbed on rough dielectric surfaces is largely governed by the opposing effects of local field enhancement and of surface induced damping.[4] The latter effect is easily calculated for flat surfaces within local electromagnetic theory.[5] Recent progress with nonlocal electromagnetic response of metal surfaces has made it possible to estimate also nonlocal effects on lifetimes of excited molecules near flat surfaces.[6,7] Calculations for rough surfaces have so far been limited to small roughness within the local electromagnetic theory,[8] while for molecules adsorbed on surfaces with large scale roughness (e.g., surface island films) we have used results of model calculations involving a molecule located near a single small dielectric spheroid.[2(a)]

In this paper we present a formalism for calculating the optical properties of molecules adsorbed on (or within) aggregates of dielectric particles, and use it to calculate the lifetimes of excited states of such molecules. The results of such calculations make it possible to analyze the error associated with approximating a molecule adsorbed on a surface with large scale roughness (e.g., surface island film) by a model consisting of a molecule and a single dielectric grain, and they also give us estimates of the lifetimes of excited molecules adsorbed on aggregates of colloid particles.

There have been in recent years a number of works which deal with the optical properties of aggregates of dielectric particles. Earlier works[9] have used a very simple model which approximates each such particle by a point dipole.[10] In later work higher multipole effects have been shown both experimentally[11] and theoretically[12,13] to be important. In this paper we extend the theoretical framework developed by Bergman[14] for calculating the electromagnetic resonances in a system of interacting dielectric grains. This framework enables us to calculate, in the long wavelength ("electrostatic") limit, the response of such a system to an oscillating point dipole which represents the excited molecule. From this we may extract the radiative and nonradiative decay rate of such a molecule by standard methods which are reviewed below. The formalism incorporates the electromagnetic interaction between the molecule and the dielectric grains and between the dielectric grains in any desired order in the multiple expansion. It is possible then to truncate this expansion in different orders and thus check the convergence of the procedure.

Even though the formalism may be extended to the short wavelength limit[15] we have limited ourselves to the long wavelength (electrostatic) limit which, for grains small relative to the radiation wavelength, should be a good approximation. This limits us also to situations where the distance between grains is small, however the main effects on the lifetimes occur for molecules close ($\leqslant$100 Å) to the dielectric surface and if the grains are

a) Supported in part by the U.S.–Israel Binational Science Foundation, Jerusalem, Israel, and by NSF grant CHE83-17098 and NSF (MRL) facilities at the University of Chicago.

 0021-9606/85/083831-10$02.10

far from each other a model that disregard all but one of them (the closest to the molecule) should be sufficient.

In what follows we first present the formal approach and then study and discuss some particular examples.

II. FORMALISM

Consider a system consisting of N phases characterized by dielectric functions $\epsilon_i(\omega)$, $i = 1 \cdots N$. Following Bergman[14] we introduce the functions $\theta_i(\mathbf{r})$ such that $\theta_i(\mathbf{r}) = 1$ if $\mathbf{r}$ is in phase i and $\theta_i(\mathbf{r}) = 0$ otherwise. Therefore,

$$\epsilon(\mathbf{r}) = \sum_{i=1}^{N} \epsilon_i \theta_i(\mathbf{r}). \tag{1}$$

Later on we consider the special case where the phases $1 \cdots N-1$ are particles embedded in phase N. Define

$$u_i = 1 - \epsilon_i/\epsilon_N; \quad i = 1 \cdots N-1. \tag{2}$$

A charge distribution $\rho(\mathbf{r})$ (later taken to be located in phase N) gives rise to an induced potential $\Psi(\mathbf{r})$ which satisfies

$$\nabla \cdot [\epsilon(\mathbf{r}) \nabla \Psi(\mathbf{r})] = 4\pi\rho(\mathbf{r}). \tag{3}$$

Using Eq. (1), Eq. (3) may be recast in the form

$$\nabla^2 \Psi = \sum_{i=1}^{N-1} u_i \nabla \cdot (\theta_i \nabla \Psi) - \frac{4\pi}{\epsilon_N} \rho. \tag{4}$$

Introducing the Green's function $G(\mathbf{r}|\mathbf{r}')$,

$$\nabla^2 G(\mathbf{r}|\mathbf{r}') = -\delta(\mathbf{r} - \mathbf{r}'), \tag{5a}$$

which for an infinite system is

$$G(\mathbf{r}|\mathbf{r}') = \frac{1}{4\pi(\mathbf{r} - \mathbf{r}')}. \tag{5b}$$

Equation (4) is written as an integral equation

$$\Psi(\mathbf{r}) = u_1 \int d^3r\, \Theta(\mathbf{r}') \nabla' G(\mathbf{r}|\mathbf{r}') \cdot \nabla' \Psi(\mathbf{r}') + \frac{1}{\epsilon_N} \Psi_\rho(\mathbf{r}), \tag{6}$$

where

$$\Theta(\mathbf{r}) = \sum_{i=1}^{N-1} (u_i/u_1) \theta_i(\mathbf{r}) \tag{7}$$

and where

$$\Psi_\rho(\mathbf{r}) \equiv 4\pi \int d^3r'\, G(\mathbf{r}|\mathbf{r}') \rho(\mathbf{r}') \tag{8}$$

is the potential at $\mathbf{r}$ due to the charge distribution ρ. We define the scalar product of any two real functions by

$$\langle \Phi | \Psi \rangle = \int d^3r\, \Theta(\mathbf{r}) \nabla \Phi^* \cdot \nabla \Psi \tag{9}$$

and the operator $\hat{G}$,

$$\hat{G}\Psi = \int d^3r'\, \Theta(\mathbf{r}') \nabla' G(\mathbf{r}|\mathbf{r}') \cdot \nabla' \Psi(\mathbf{r}'), \tag{10}$$

so that

$$\langle \Phi | \hat{G} | \Psi \rangle = \int d^3r \int d^3r'\, \Theta(\mathbf{r}) \Theta(\mathbf{r}') \nabla \Phi^*(\mathbf{r}) \times \nabla \nabla' G(\mathbf{r}|\mathbf{r}') \cdot \nabla' \Psi(\mathbf{r}'). \tag{11}$$

Equations (9)–(11) constitute a generalization to many phases of the similar definitions introduced by Bergman[14] for the two phase system. In terms of $\hat{G}$ the integral equation (6) takes the form

$$\Psi = u_1 \hat{G} \Psi + \frac{1}{\epsilon_N} \Psi_\rho. \tag{12}$$

Most of the properties of $\hat{G}$ derived for the two phase[14] system are valid also in the multiphase case. One important difference is that for the two phase system $\hat{G}$ depends only on the geometry (not on the dielectric functions) while this is no longer so in the general case. Still $\hat{G}$ is linear and is easily shown to be self-adjoint. We may conclude that its eigenfunctions form a complete orthogonal set with respect to the scalar product (9). We may therefore expand any piecewise continuously differentiable function within the space of phases $1 \cdots N-1$ in a series of these functions. Defining these eigenfunctions and the associated eigenvalues by

$$\hat{G} \Psi_\alpha = s_\alpha \Psi_\alpha \tag{13}$$

and expanding (in the region outside θ_N)

$$\Psi = \sum_\alpha C_\alpha \Psi_\alpha, \tag{14a}$$

$$\Psi_\rho = \sum_\alpha D_\alpha \Psi_\alpha, \tag{14b}$$

we get a formal solution of Eq. (12) in this region in the form

$$C_\alpha = \frac{D_\alpha}{\epsilon_N (1 - u_1 s_\alpha)}. \tag{15}$$

This is in general not a useful approach since the main difficulty is in solving the eigenvalue problem (13). Instead we follow Bergman in using an expansion in the eigenfunctions of individual grains. We consider a system where phases $1 \cdots N-1$ constitute grains which are distributed in phase N. Consider one such grain, a, with dielectric function ϵ_a imbedded in an otherwise pure infinite medium made of phase N. The corresponding Green's operator is defined by

$$\hat{G}_a \Psi = \int d^3r'\, \theta_a(\mathbf{r}') \nabla' G(\mathbf{r}|\mathbf{r}') \cdot \nabla' \Psi(\mathbf{r}') \tag{16}$$

and its eigenfunctions $\Psi_{a\alpha}$ and eigenvalues $s_{a\alpha}$ ($\hat{G}_a \Psi_{a\alpha} = s_{a\alpha} \Psi_{a\alpha}$) are easily shown to satisfy

$$\nabla \cdot \left\{ \left[\left(1 - \frac{1}{s_{a\alpha}} \right) \theta_a + \theta_N \right] \nabla \Psi_{a\alpha} \right\} = 0. \tag{17}$$

Equation (17) has the form of a Laplace equation for the electrostatic field in a system consisting of grain a in medium N provided we identify $1 - 1/s_{a\alpha}$ with ϵ_a/ϵ_N. The eigenvalues $s_{a\alpha}$ correspond to such values of ϵ_a/ϵ_N for which a field ($\nabla \Psi_{a\alpha}$) may exist in the grain in the absence of any external source. These solutions are well known for grains of simple shapes, e.g., ellipsoids. For a sphere of radius r_a we get

$$\Psi_{lm}(\mathbf{r}) = \begin{cases} (lr_a^{2l+1})^{-1/2} r^l Y_{lm}(\Omega) & r \leqslant r_a \\ (lr_a^{2l+1})^{-1/2} \dfrac{r_a^{2l+1}}{r^{l+1}} Y_{lm}(\Omega) & r \geqslant r_a, \end{cases} \tag{18}$$

$$s_{lm} = l/(2l+1), \tag{19}$$

where the collective index α is here determined by $l = 0, 1, 2\cdots$ and $m = -l, -l+1\cdots l$. $\Omega = (\theta, \rho)$ is the spherical angle and $Y_{lm}(\Omega)$ are the spherical harmonics. The normalization in Eq. (18) is chosen so that

$$\langle \Psi_{lm} | \Psi_{l'm'} \rangle = \delta_{ll'}\delta_{mm'}. \tag{20}$$

For a system consisting of grains distributed in phase N we may expand the potential Ψ in each grain in terms of the grain eigenfunctions. To this end define θ_a^+ as a step function which is unity in a volume infinitesimally larger than grain a (so that $\nabla\theta_a = 0$ in grain a and on its surface) and define also

$$\eta = \sum_{a=1}^{N-1} \theta_a = 1 - \theta_N, \tag{21a}$$

$$\eta^+ = \sum_{a=1}^{N-1} \theta_a^+. \tag{21b}$$

Note that $\hat{G}$ may be represented by

$$\hat{G} = \sum_{a=1}^{N-1} (u_a/u_1)\hat{G}_a \tag{22}$$

and that $\hat{G}_a$ and $\hat{G}$ satisfies the relations

$$\hat{G}_a = \hat{G}_a\theta_a^+, \tag{23a}$$

$$\hat{G} = \hat{G}\eta^+. \tag{23b}$$

Consider now the projection of Eq. (12) on the subspace defined by η^+:

$$\eta^\perp\Psi = u_1\eta^+\hat{G}\Psi + \frac{1}{\epsilon_N}\eta^+\Psi_\rho. \tag{24}$$

Using Eqs. (21)–(23) this implies

$$\theta_a^+\Psi = \theta_a^+ \sum_{b=1}^{N-1} u_b\hat{G}_b\theta_b^+\Psi + \frac{1}{\epsilon_N}\theta_a^+\Psi_\rho. \tag{25}$$

For each grain expand

$$\theta_a^+\Psi = \sum_\alpha C_{a\alpha}\theta_a^+\Psi_{a\alpha}, \tag{26a}$$

$$\theta_a^+\Psi_\rho = \sum_\alpha D_{a\alpha}\theta_a^+\Psi_{a\alpha}. \tag{26b}$$

Inserting Eq. (26) into Eq. (25) and taking a scalar product with a particular $\Psi_{a\alpha}$ yields

$$C_{a\alpha} = \frac{1}{\epsilon_N}D_{a\alpha} + \sum_{b\beta} Q_{a\alpha;b\beta}C_{b\beta}, \tag{27}$$

where

$$Q_{a\alpha;b\beta} = u_b S_{b\beta} \int d^3r\, \theta_a(\mathbf{r})\nabla\Psi^*_{a\alpha}(\mathbf{r})\cdot\nabla\Psi_{b\beta}(\mathbf{r}). \tag{28}$$

Note that the orthonormality condition on functions defined on the same grain implies that $Q_{a\alpha;a\beta} = u_b s_\alpha \delta_{\alpha\beta}$. Defining the vectors $\mathbf{C}$ and $\mathbf{D}$ with elements $\{C_{a\alpha}\}$ and $\{D_{a\alpha}\}$ and the matrix $\mathbf{Q} = \{Q_{a\alpha;b\beta}\}$ we get

$$\mathbf{C} = \frac{1}{\epsilon_N}(\mathbf{I} - \mathbf{Q})^{-1}\mathbf{D}, \tag{29}$$

where $\mathbf{I}$ is the unit matrix. This is the required formal solution for $\mathbf{C}$ in terms of the presumably known vector $\mathbf{D}$ and matrix $\mathbf{Q}$. In the Appendix we summarized the necessary formulas for the elements of $\mathbf{D}$ and of $\mathbf{Q}$ in the case where the grains are spheres and the inducing charge distribution is a point dipole.

The solution $\mathbf{C}$ obtained from Eq. (29) corresponds to the potential within the grains. It is also possible to evaluate the potential in phase N. To do this we return to Eq. (12) and use Eq. (23b) to write it in the form

$$\Psi = u_1\hat{G}\eta^+\Psi + \frac{1}{\epsilon_N}\Psi_\rho. \tag{30}$$

Using Eqs. (21b), (22), (23a), and (26a) we get from Eq. (30):

$$\Psi = \frac{1}{\epsilon_N}\Psi_\rho + \sum_{a=1}^{N-1} u_a \sum_\alpha C_{a\alpha}s_{a\alpha}\Psi_{a\alpha}. \tag{31}$$

Thus after having found $C_{a\alpha}$ (and Ψ within the grains) from Eq. (29), the potential Ψ everywhere may be found from Eq. (31). This last result is actually not needed for calculating the radiationless and radiative decay rates of the adsorbed molecule, as shown below.

We now calculate these decay rates for the case where the charge distribution ρ is a point dipole and where the phase N is characterized by $\epsilon_N = 1$. For this we use the procedure used by Gersten and Nitzan for evaluating optical properties of a molecule near a single dielectric particle. We first focus on the nonradiative decay. This results from energy loss due to heat generated in the dissipative phases of the grains. The rate of heat generation is for a field oscillating with frequency ω:

$$\left(\frac{dW}{dt}\right)_{\mathrm{NR}} = \frac{1}{2}\int d^3r\, \sigma(\mathbf{r})|\nabla\Psi(\mathbf{r})|^2, \tag{32}$$

where

$$\sigma(\mathbf{r}) = \frac{\omega}{4\pi}\,\mathrm{Im}[\epsilon(\mathbf{r})] \tag{33a}$$

is the conductivity at $\mathbf{r}$. Rewriting σ as

$$\sigma(\mathbf{r}) = \frac{\omega}{4\pi}\sum_{a=1}^{N-1}\mathrm{Im}[\epsilon_a\theta_a(\mathbf{r})] \tag{33b}$$

and using the expansion (26a) for each grain together with the orthonormality property $\langle\Psi_{a\alpha}|\Psi_{a\beta}\rangle = \delta_{\alpha\beta}$ we obtain from Eq. (32),

$$\frac{dW}{dt} = \frac{\omega}{8\pi}\sum_{a\alpha}|C_{a\alpha}|^2\,\mathrm{Im}[\epsilon_a(\omega)]. \tag{34}$$

This is the heat generated in the dielectric grains due to

the presence of the source dipole which oscillates with frequency ω. For the latter we adopt a simple harmonic oscillator model which implies the following relationship between the dipole amplitude μ_0, its static polarizability α_0, and the energy W[16]:

$$W = \frac{\mu_0^2}{2\alpha_0}. \tag{35}$$

The polarizability α_0 is related to the radiative decay rate $\Gamma_R^{(f)}$ of the free molecule

$$\alpha_0 = \frac{3}{2}\frac{\Gamma_R^{(f)}}{\omega}\left(\frac{c}{\omega}\right)^3, \tag{36}$$

where c is the speed of light. Using Eqs. (34)–(36), the nonradiative decay rate $\Gamma_{NR} = W^{-1}(dW/dt)$ takes the final form

$$\Gamma_{NR} = \frac{3}{8\pi}\left(\frac{c}{\omega}\right)^3\left[\sum_{a=1}^{N-1}\sum_{\alpha}\frac{|C_{a\alpha}|^2}{\mu_0^2}\,\mathrm{Im}[\epsilon_a(\omega)]\right]\Gamma_R^{(f)}. \tag{37}$$

It should be noted that $|C_{a\alpha}|^2/\mu_0^2$ is independent of μ_0 as implied by Eqs. (26b) and (29).

Turning now to the evaluation of the radiative decay rate, we start with the classical expression for the rate of radiative energy loss from a dipole of amplitude μ_0^{tot} oscillating with frequency ω:

$$\frac{dW}{dt} = \frac{1}{3}c\left(\frac{\omega}{c}\right)^4|\mu_0^{tot}|^2. \tag{38}$$

Here μ_0^{tot} is the amplitude of the total dipole induced in the system. Equations (35), (36), and (38) lead to an expression for the radiative decay rate

$$\Gamma_R = \frac{|\mu_0^{tot}|^2}{|\mu_0|^2}\Gamma_R^{(f)}. \tag{39}$$

μ_0^{tot} is given by

$$\mu_0^{tot} = \mu_0 + \sum_a \frac{\epsilon_a - 1}{4\pi}\int d^3r\,\theta_a(\mathbf{r})\mathbf{E}(\mathbf{r}). \tag{40}$$

To evaluate the integral

$$I = \int d^3r\,\theta_a(\mathbf{r})\mathbf{E}(\mathbf{r}) = -\int d^3r\,\theta_a(\mathbf{r})\nabla\Psi(\mathbf{r}), \tag{41}$$

we consider its components, e.g.,

$$I_x = -\int d^3r\,\theta_a(\mathbf{r})\nabla\Psi\cdot\nabla x, \tag{42}$$

where $\nabla x = \hat{n}_x$ is a unit vector in the x direction. Next we note that the functions Ψ and x in Eq. (42) may be expanded in the volume of the grain a:

$$\theta_a^+\Psi = \sum_\alpha C_{a\alpha}\theta_a^+\Psi_{a\alpha}(\mathbf{r}), \tag{43a}$$

$$\theta_a^+ x = \sum_\alpha F_{a\alpha}^{(x)}\theta_a^+\Psi_{a\alpha}(\mathbf{r}). \tag{43b}$$

Note that Ψ and x are real, however $C_{a\alpha}$, $F_{a\alpha}^{(x)}$, and $\Psi_{a\alpha}$ need not be so. Inserting Eq. (43) into Eq. (42) we get

$$I_x = -\sum_\alpha C_{a\alpha}^* F_{a\alpha}^{(x)} \tag{44}$$

and similarly for the y and z components. Inserting $I = \hat{n}_x I_x + \hat{n}_y I_y + \hat{n}_z I_z$ into Eq. (40) we finally obtain

$$\mu_0^{tot} = \mu_0 - \sum_a \frac{\epsilon_a - 1}{4\pi}\sum_\alpha C_{a\alpha}^*(\hat{n}_x F_{a\alpha}^{(x)} + \hat{n}_y F_{a\alpha}^{(y)} + \hat{n}_z F_{a\alpha}^{(z)}). \tag{45}$$

Equations (39) and (45) constitute our final results for the radiative decay rate. This seemingly complicated expression is greatly simplified for the case of ellipsoidal particles for which expansions like Eq. (43b) are simple (particularly if the axes are chosen along the principal axes of the particle). Thus, for a sphere of radius r_a the functions $x = r\sin\theta\cos\varphi$, $y = r\sin\theta\sin\varphi$ and $z = r\cos\theta$ ($r < r_a$) are easily expressed in terms of the functions $\Psi_{lm}(\mathbf{r})$, $l = 1$, $m = 0, \pm 1$ (Eq. 18):

$$x = -\sqrt{\frac{2\pi}{3}}\,r_a^{3/2}(\Psi_{1,1} - \Psi_{1,-1}),$$

$$y = i\sqrt{\frac{2\pi}{3}}\,r_a^{3/2}(\Psi_{1,1} + \Psi_{1,-1}),$$

$$z = \sqrt{\frac{4\pi}{3}}\,r_a^{3/2}\Psi_{10}. \tag{46}$$

Using Eqs. (43b) and (46) to obtain the coefficients $F_{alm}^{(k)}$ ($k = x, y, z$), then using Eqs. (39) and (45), we arrive at the following result for the radiative decay rate of a molecule (represented by a point dipole):

$$\Gamma_R = \Gamma_R^{(f)}\left\{\left|\sin\theta\cos\varphi + \sqrt{\frac{2\pi}{3}}\sum_a\frac{\epsilon_a - 1}{4\pi}\,r_a^{3/2}(\tilde{C}_{a,1,1} - \tilde{C}_{a,1,-1})\right|^2\right.$$

$$\left. + \left|\sin\theta\sin\varphi + i\sqrt{\frac{2\pi}{3}}\sum_a\frac{\epsilon_a - 1}{4\pi}\,r_a^{3/2}(\tilde{C}_{a,1,1} + \tilde{C}_{a,1,-1})\right|^2 + \left|\cos\theta - \sqrt{\frac{4\pi}{3}}\sum_a\frac{\epsilon_a - 1}{4\pi}\,r_a^{3/2}\tilde{C}_{a,1,0}\right|^2\right\}, \tag{47}$$

where $\tilde{C} = C/\mu_0$ and where θ and φ denote the direction of the molecular dipole in space.

In the next section we apply the results of this section to the calculation of the radiative Γ_R and the nonradiative Γ_{NR} decay rates, as well as the emission yield

$$Y = \frac{\Gamma_R}{\Gamma_R + \Gamma_{NR}} \tag{48}$$

of a molecule represented by a point dipole which is located in the vicinity of spherical dielectric grains.

III. DECAY RATES OF A MOLECULE NEAR A SYSTEM OF DIELECTRIC SPHERES

In this section we present detailed calculations for the lifetimes and quantum yield associated with a point dipole in a system of polarizable spheres. These lifetimes are given by Eqs. (37) and (47) in terms of the coefficients $C_{a\alpha}$ [$\alpha = (l, m)$], which are obtained from Eq. (28). To get these coefficients we need explicit expressions for the elements of the vector **D** and the matrix **Q** defined by Eqs. (26b) and (28), respectively. Such expressions are given in the Appendix. Since **Q** and **D** are infinite, corresponding to the infinite number of multipoles ($l = 0, 1, \cdots; m = -l \cdots +l$), we truncate the multipole expansion at some $l = L$ while testing for convergence by comparing results obtained for different values of L. This truncation should be done with caution though, because when the dipole is close to one of the spheres (i.e., when $d \ll r_a$ where d is the distance of the dipole from the sphere surface and r_a the sphere radius) the image potential seen by the dipole (which makes most of the contribution to the nonradiative lifetime) is a very slowly convergent series if expressed in terms of multipole moments. Typically several hundred moments are needed to give a good representation of the image field felt by a dipole located at $d \leqslant 0.05 r_a$. We therefore adopt the following truncation procedure: for all spheres we take into account all multipole moments with $l \leqslant L$ (in the calculations reported below $L \leqslant 8$) and the couplings $Q_{alm;bl'm'}$ between them. For the sphere, a, closest to the dipole we take also higher multipole contributions (for the smallest distance considered by us, $d = 5$ Å, on a sphere radius of 100 Å, we have to sum terms up to $l \sim 750$ in order to get the image with less than 1% error). However, the nondiagonal elements of **Q** which couple these higher multipoles to the multipole moments of other spheres are disregarded. Therefore the matrix **I** − **Q** of Eq. (28) contains a relatively small nondiagonal part, which is inverted numerically, and a large diagonal part.

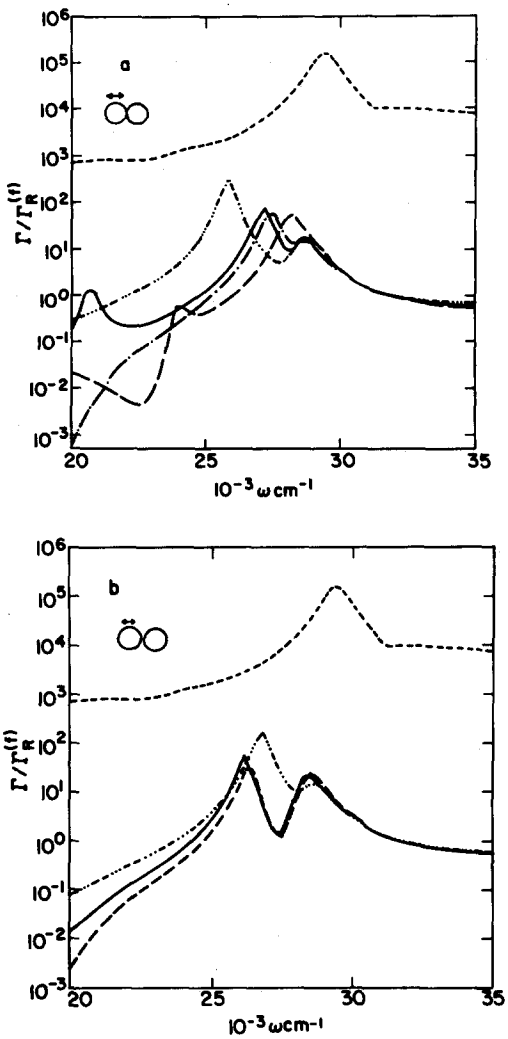

FIG. 1. Radiative and nonradiative relaxation rates (relative to the free molecule radiative decay rate) of a molecule adsorbed on a two-sphere silver cluster. The inset shows the geometry of the system where the double arrow denotes the orientation of the (point) molecular dipole. ---: surface induced nonradiative relaxation rate. This result does not depend on L. The other curves are radiative decay rates obtained for $L = 2$ (-· · -· · -· ·), $L = 4$ (---), $L = 7$ (-·-·-·-·) and $L = 8$ (—). The molecule lies along the line perpendicular to the intersphere axis and passing through a sphere center at a distance of 1.1 from this center. In Fig. 1(a) the spheres are touching. In Fig. 1(b) the distance between their centers is 2.2. All distances are in units of the sphere radius which was taken to be 100 Å. In Fig. 1(b) the lines corresponding to $L = 7$ and $L = 8$ lie on top of each other.

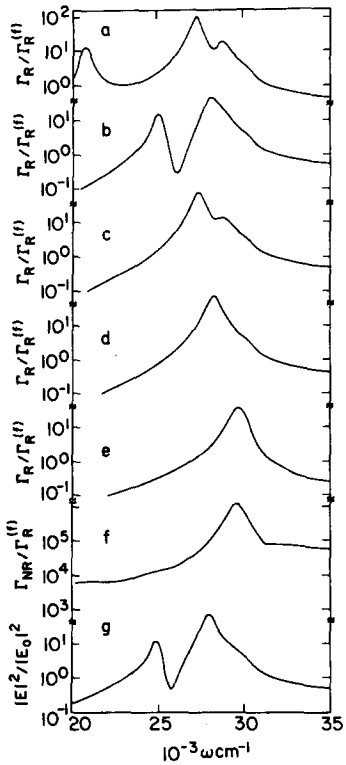

FIG. 2. Optical properties of a molecule located near silver surfaces of different configuration. (a)–(c) Radiative decay rate of a molecule near a two-sphere cluster in a configuration similar to that of Fig. 1. The distance between the molecule and the center of the nearest sphere is 1.05. The distance between the sphere centers is 2.0 (a), 2.1 (b), and 2.5 (c). Note that the result for $\omega < 23\,000$ cm^{-1} in (a) is not reliable because of lack of convergence in this range. (d) Radiative decay rate of a molecule located at a distance 1.05 from the center of a single sphere. (e) Radiative decay rate of a molecule near a plane (for distances much smaller than the radiation wavelength $2\pi c/\omega$, where c is the speed of light, this rate is distance independent). (f) Nonradiative decay rate of a molecule in a situation similar to that of (b). This result does not depend on the intersphere distance. In (a)–(f) the molecular dipole is parallel to the nearest surface. (g) Local field enhancement $|E|^2/|E_0|^2$ at the position of the molecule in the configuration of (b). The incident field E_0 is parallel to the bispherical axis and the local field E is measured in the same direction.

The results reported below address first the question of convergence of this truncation procedure and then the following physical questions:

(a) How do the lifetimes (radiative and nonradiative) of a molecule located near a rough surface, represented

by a cluster of dielectric (spherical) grains, depend on the morphology of the substrate. In particular, to what extent do plan geometry and a single grain model constitute good approximations for estimating these lifetimes?

(b) Modeling a very rough surface as a plane of spheres—how do the relaxation times depend on the molecule's distance from this plane as compared to the smooth surface and the single sphere case?

(c) How does the surface (or cluster) structure affect the frequency dependence of the relaxation rates?

(d) How do the features mentioned above behave for different molecule locations and orientations relative to the grains?

For the calculation reported below we have considered (unless otherwise stated) silver grains (using the bulk dielectric function of silver from Ref. 17) in vacuum. All the distances reported are in units of the sphere radius which was taken to be 100 Å.

Figure 1 displays the radiative and nonradiative relaxation rates (relative to $\Gamma_R^{(0)}$, the radiative decay rate of the free molecule) for a molecule adsorbed on a two sphere cluster (the geometry of the system is shown in the inset) as a function of molecular frequency. We show results of calculations based on different truncation schemes (with maximum multipole order $L = 2$, 4, 7, and 8). However, for all cases the interaction between the molecular dipole and the nearest sphere was calculated up to order $L = 750$ which gave the correct image even for the small molecule-sphere surface distances considered.

For the case of touching spheres [Fig. 1(a)] convergence of the radiative decay rate is seen to be slow. However, going from $L = 7$ to $L = 8$ is seen to make little difference for $\omega > 3$ eV. When the spheres are slightly apart [Fig. 2(b)] convergence is much more rapid, and for an intersphere distance of 2.2 is practically achieved for $L = 7$. The nonradiative decay rate is not affected by the order of the calculation since most of the contribution to it is due to the nearest sphere whose coupling with the molecular dipole is taken to order $L = 750$.

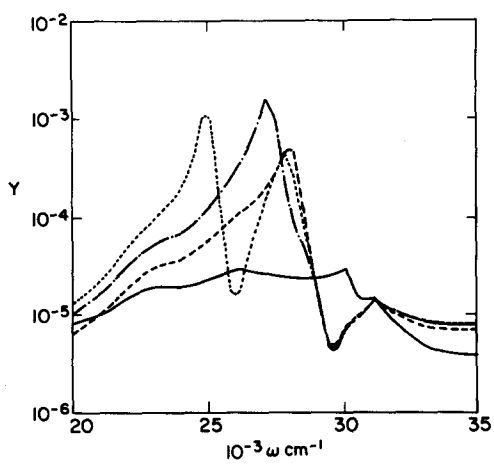

FIG. 3. Quantum yield Y for emission from a molecule located near different silver surfaces. The molecule is assumed to have $Y = 1$ when free. —: a molecule at a distance 5 Å from a plane surface; ---: a molecule at a distance 5 Å from a single sphere surface. The sphere radius is 100 Å; · · ·: a molecule near a two-sphere cluster in the configuration of Fig. 1. The distance between the sphere centers is 2.1 radii; -·-·-·: same with the distance between sphere centers 2.5.

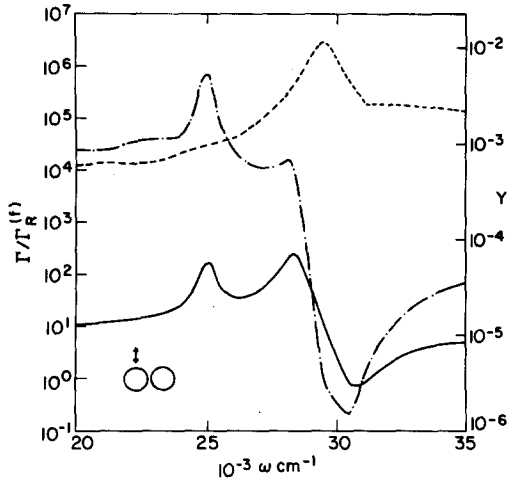

FIG. 4. Radiative decay rate (—), surface induced nonradiative decay rate (---) and emission yield (-·-·-·) for a molecule near a two-sphere cluster. The configuration is shown in the inset. The distance between the molecule and the center of nearest sphere is 1.05.

Figure 2 shows as a function of molecular frequency the radiative and nonradiative relaxation rates of a molecular dipole lying near a two sphere cluster along the nearest sphere radius which is normal to the bispherical axis. The molecular dipole is parallel to this axis (configuration similar to that of Fig. 1). The distance between the molecule and the center of the nearest sphere is 1.05. Different calculations corresponding to different intersphere distances as well as to the molecule near a plane case shown. Figure 3 displays the quantum yields calculated for these different cases. In all these cases the calculation was truncated at $L = 8$.

These calculations show that the radiative lifetime (hence the quantum yield) is quite sensitive to the cluster structure (expressed here in terms of the distance between the spheres). On the other hand, the nonradiative lifetime is quite insensitive to this structure as long as the molecule is predominantly affected by one grain. The reason for this, as discussed above, is that the surface induced damping results from relatively short range image effects which are largely dominated by the nearest sphere.

The structure in the molecular frequency dependence of the radiative decay rate is determined by the resonances in the dielectric response of the spheres system. This may be seen by comparing Fig. 2(b) to Fig. 2(g) which displays the local electric field in the vicinity of the two sphere system due to an incident spatially independent field $\mathbf{E}_0 e^{i\omega t}$ whose direction is parallel to the bispherical axis. These resonances are sensitive to the cluster structure because they are influenced by the interactions and the interferences between the charge distributions induced on the different spheres.

In Figs. 4 and 5 we show the results of calculations similar to those done in Figs. 2 and 3 but for different molecular positions and orientations. These results should be compared to the single sphere (Fig. 6) and the plane

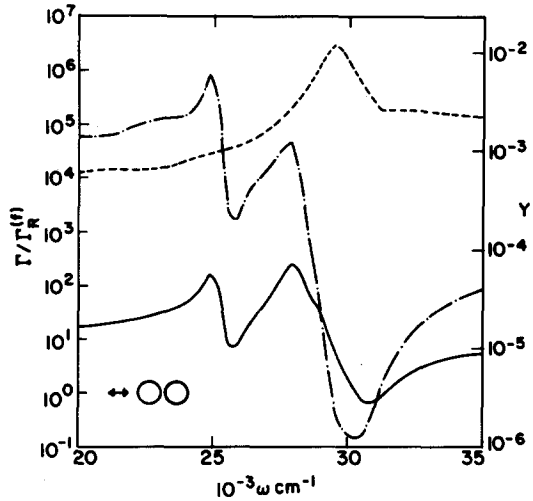

FIG. 5. Same as Fig. 4 with another configuration as shown in the inset.

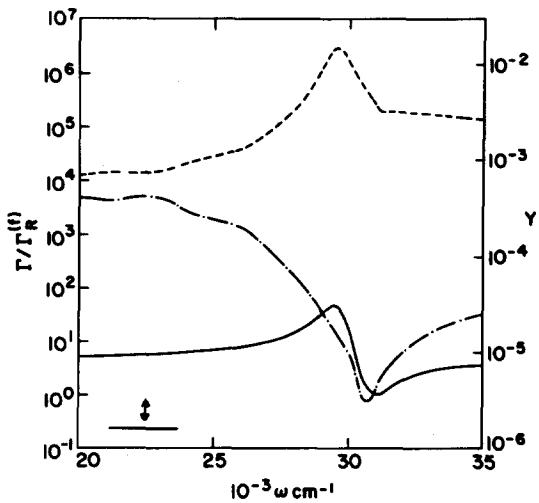

FIG. 7. Same as Fig. 4 for a molecule at distance 5 Å from a plane surface in a perpendicular orientation.

(Fig. 7) results. All the calculations described above which involve two spheres use a truncated multipole expansion with $L = 8$.

In Figs. 8 and 9 similar results are shown for a molecule located above a cluster of five silver spheres which may be thought of as part of a two-dimensional square periodic array of spheres. The molecule is seated in a perpendicular orientation on the line passing through the center of the central sphere perpendicular to the plane of the spheres. In these calculations we truncate the multipole expansion at $L = 4$. Convergence is achieved at this order because of the larger distance between the spheres. Two features should be pointed out: First, it is seen that the resonance structure obtained for this configuration is broader and smoother than that obtained for the two sphere system. This is probably due to the overlap between several peaks originated from the interactions between the resonances associated with the different spheres. Secondly, note that as the distance between the molecule and the cluster increases the nonradiative relaxation rate becomes more sensitive to the cluster structure since it is less dominated by the interaction with the nearest sphere. This is seen more clearly in Fig. 10 where the radiative and nonradiative relaxation rates of a molecule characterized by $\omega = 26\,200\ cm^{-1}$ are plotted for a geometry similar to that of Figs. 8 and 9 as a function of the lattice constant—the distance between the spheres centers. It is interesting to note that the radiative decay rate increases when the cluster comes apart. This is due to the fact that for this configuration the dipole induced on the central sphere is different in sign than those induced on the other four spheres so the proximity of these other spheres reduces the total and hence the radiative emission rate. This observation has implications also for the lifetime of a molecule imbedded in a cluster

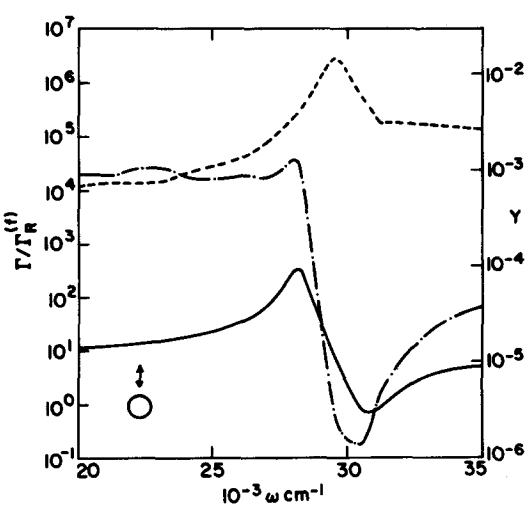

FIG. 6. Same as Fig. 4 for a molecule near a single sphere. The molecule is perpendicular to the sphere surface and is located at distance 1.05 from the sphere center.

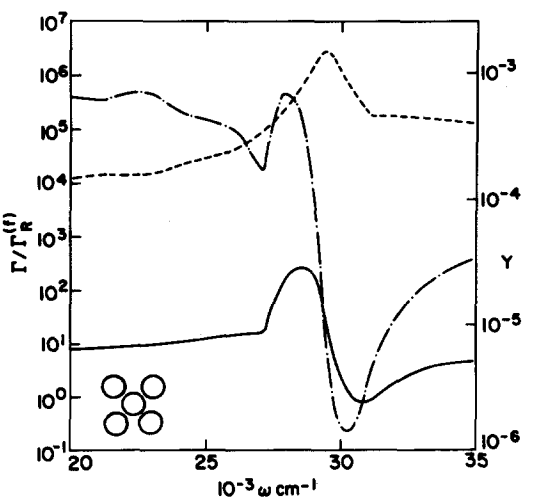

FIG. 8. Radiative decay rate (—), surface induced nonradiative decay rate (---) and emission yield (-·-·-·-) for a molecule located above a plane containing five silver spheres. The sphere arrangement is shown in the inset. The distances between the sphere centers are all 2.5. The molecule is seated in a perpendicular orientation on the normal to the plane of spheres which passes through the center of the central sphere at a distance of 1.05 from this center.

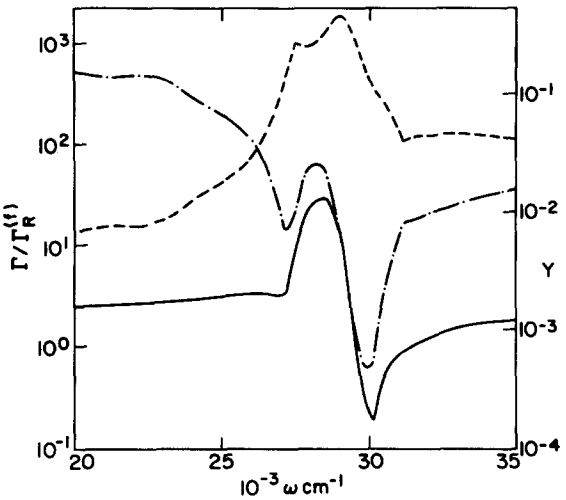

FIG. 9. Same as Fig. 8 with the distance of the molecule from the plane of sphere centers is now 1.5.

of polarizable atoms or molecules as will be discussed elsewhere.[18]

Finally, in Fig. 11 we give the dependence of the molecular relaxation rates and quantum yield on the molecule distance from the plane of spheres in the geometry of Figs. 8–10. In Figs. 11(a), 11(b), and 11(c) we compare the distance dependence of the radiative and nonradiative decay rates and of the quantum yields for the cases of a molecule (of $\omega = 26\,200\ cm^{-1}$) above the 5 sphere plane, a single sphere and a smooth plane, respectively. Substantial differences are observed between these cases.

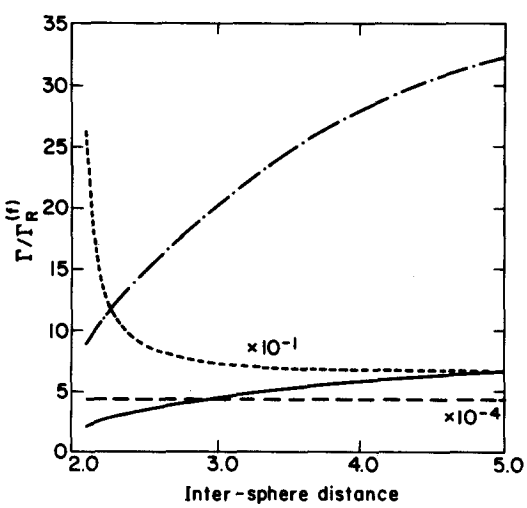

FIG. 10. Radiative and nonradiative relaxation rates of a molecule located above a five-sphere planar cluster in the configuration of Fig. 8 as a function of distance between the sphere centers (express in units of the sphere radius). The molecule is represented by a point polarizable particle with characteristic resonance frequency $\omega = 26\,200\ cm^{-1}$ (corresponding for silver to a dielectric constant $\epsilon = -3.5 + 0.19i$ (—): Radiative relaxation rate for a molecule located above the central sphere at a distance 1.5 from its center. (---): Nonradiative decay rate for the same molecule (-·-·-·): Radiative relaxation rate for a molecular-central sphere distance 1.05. (--): Nonradiative relaxation rate for the same molecule.

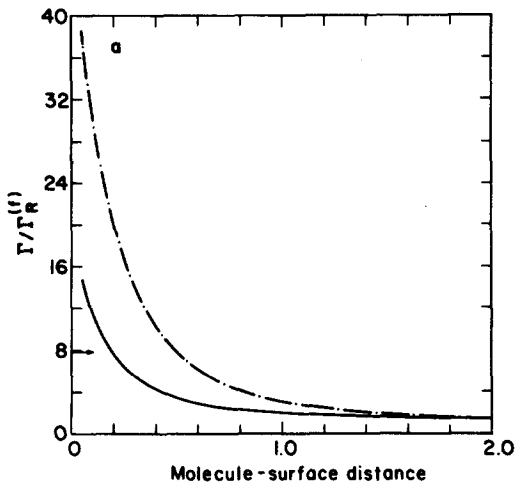

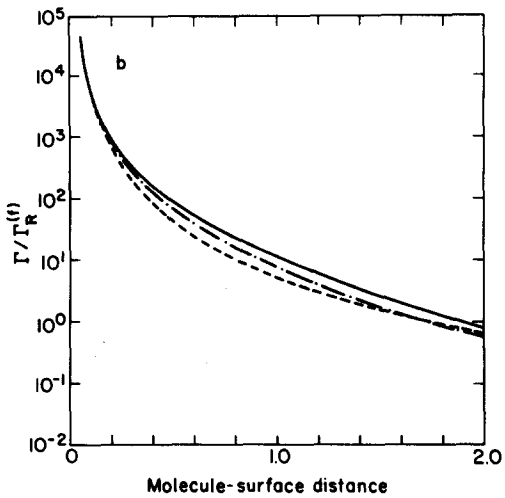

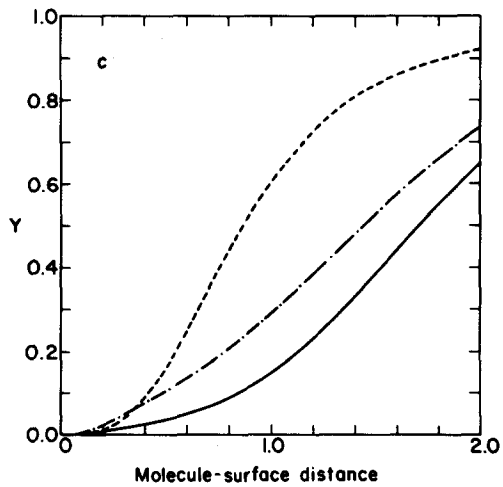

FIG. 11. (a) (—): Radiative decay rate of a molecule above a five-sphere planar cluster in the configuration of Fig. 8 as a function of the distance between the molecule and the cluster plane. (-·-·-·): same for a molecule near a single sphere. The molecular dipole orientation is perpendicular to the nearest surface and the molecule is characterized by $\omega = 26\,200\ cm^{-1}$. The arrow marks the value of the radiative decay rate for this molecule near a planar surface (which is distance independent for distances small relative to the radiation wavelength). (b) Same for the nonradiative decay rate induced by the spheres (—): five-sphere cluster in the configuration of Fig. 8; (-·-·-·): single sphere; (---): plane. (c). Same as (b) for the emission yield $Y = \Gamma_R/(\Gamma_R + \Gamma_{NR})$.

IV. CONCLUSIONS

In this paper we have developed a general method for calculating radiative and surface induced nonradiative decay rates of molecules adsorbed on clusters of dielectric grains and have used it to study these phenomena for the particular case of spherical grains. Our results constitute a generalization of previous studies of the same phenomena for a molecule on a planar surface and on a single dielectric grain.

Obviously the detailed results described in the previous section serve only to describe the scope of these phenomena and are not expected to be directly measurable. The dependence of the rates and quantum yield on morphological details and on molecular location and orientation relative to the grains indicate that, as intuitively expected, there should be a broad distribution of lifetimes and yields in such systems. Since different positions and orientations explore different dielectric resonances of the cluster this distribution may be very broad indeed. We should keep in mind however that for large coverages fast energy transfer between the adsorbed molecules may have the effect of practically narrowing this lifetime distribution. Furthermore, since the lifetime is seen to be dominant by the surface induced nonradiative relaxation and since this decay channel is the least sensitive to the cluster structure (excluding cases where the molecule is adsorbed in the space bordering two or more grains), the distribution of total decay rates will be much narrower than that of the radiative decay rates. This is true as long as the system is made of only one dielectric substrate.

This last conclusion is also relevant for evaluating the efficiency of photochemical and some photophysical processes involving molecules adsorbed on rough structures as those considered here. Such processes are dominated by the competition between the local field enhancement and the surface induced damping. We have seen that the latter could be accurately estimated for adsorbate molecules in the first monolayer from a single sphere or a smooth plane model, while an order of magnitude estimate may be obtained from these models even for molecules which are further away from the surface (as long as $d < r_a$, where d is the molecule surface distance and r_a is the typical scale of the roughness).

The method developed in this work may be applied also for calculating local field enhancement in clusters of dielectric grains. Using this method we have recently evaluated such enhancement factors for hidden positions within the cluster and have shown that the results of recent experiments,[19] which indicate that the largest surface enhanced Raman signals are associated with molecules which are hidden to other surface probes, may be rationalized within the electromagnetic theory of surface enhanced Raman scattering. This study will be published elsewhere.[20]

APPENDIX

Here we summarize the results for the elements $Q_{alm;bl'm'}$ and D_{alm} defined by

$$D_{alm} = \langle \Psi_{alm} | \Psi_\rho \rangle, \tag{A1}$$

$$Q_{alm;bl'm'} = u_b s_{bl'm'} \langle \Psi_{alm} | \Psi_{bl'm'} \rangle, \tag{A2}$$

where [cf. Eqs. (18) and (19)]

$$\Psi_{alm}(r, \theta, \varphi) = \begin{cases} (l r_a^{2l+1})^{-1/2} r^l Y_{lm}(\theta, \varphi) & r \leqslant r_a \quad \text{(A3)} \\ (l r_a^{2l+1})^{-1/2} \dfrac{r_a^{2l+1}}{r^{l+1}} Y_{lm}(\theta, \varphi) & r \geqslant r_a, \quad \text{(A4)} \end{cases}$$

with r, θ, φ being spherical coordinates relative to the center of sphere a. The quantity

$$\Psi_\rho(r, \theta, \varphi) = \frac{4\pi}{3} \frac{\mu}{r^2} \sum_{m=-1}^{1} q_{1m}(\theta_d, \varphi_d) Y_{1m}(\theta, \varphi) \tag{A5}$$

is the potential of a point dipole expressed in spherical coordinates r, θ, φ relative to the dipole position. θ_d and φ_d are the spherical angles characterizing the dipole orientation in the same coordinate system. The coefficients q_{lm} are given by[21]

$$q_{1,0} = \sqrt{\frac{3}{4\pi}} \cos \theta_d,$$

$$q_{1,\pm 1} = \mp \sqrt{\frac{3}{8\pi}} \sin \theta_d e^{\mp i\varphi_d}. \tag{A6}$$

Also in Eqs. (A1) and (A2),

$$s_{blm} = \frac{l}{2l+1} \quad \text{[cf. Eq. (19)]}, \tag{A7}$$

$$u_b = 1 - \epsilon_b \quad \text{[cf. Eq. (2)]}, \tag{A8}$$

and [cf. Eq. (9)]

$$\langle \Psi_{alm} | F \rangle = \int d^3r \, \theta_a(\mathbf{r}) \nabla \Psi^*_{alm}(\mathbf{r}) \cdot \nabla F(\mathbf{r}), \tag{A9}$$

where $\theta_a(r)$ is a step function which is unity in the volume of sphere, a, and is zero elsewhere.

Evaluating the integrals in Eqs. (A1) and (A2) is obviously a problem of expressing spherical functions defined about a given center in terms of spherical functions defined about another center. A general discussion and explicit solutions for this problem are given by Danos and Maximon.[22] Application of their results to our problem leads to

$$\begin{aligned} Q_{a,l,m;b,l',m'} &= u_b \cdot (-1)^{l'+m} \frac{r_a^{l+1/2} r_b^{l'+1/2}}{R_{ab}^{l+l'+1}} \left(\frac{ll'}{(2l+1)(2l'+1)} \right)^{1/2} \\ &\times \frac{(l+l'+m-m')!}{[(l+m)!(l-m)!(l'+m')!(l'-m')!]^{1/2}} \\ &\times \exp[i\varphi_{ab}(m'-m)] P_{l'+l}^{m'-m}(\cos \theta_{ab}), \\ D_{alm} &= u_b \mu_0 \sum_{m'=-1}^{1} q_{1,m'}(\theta_d, \varphi_d) \left(\frac{3l}{2l+1} \right)^{1/2} (-1)^{1+m} \frac{r_a^{l+1/2}}{R_{ad}^{l+2}} \\ &\times \frac{(1+l+m-m')!}{[(l+m)!(l-m)!(1+m')!(1-m')!]^{1/2}} \\ &\times \exp[i\varphi_{ad}(m'-m)] P_{1+l}^{m'-m}(\cos \theta_{ad}), \end{aligned} \tag{A10}$$

where R_{ab} is the distance between the centers of spheres a and b and r_a and r_b are their radii. φ_{ab} and φ_{ab} are the polar angles associated with the vector pointing from a to b, R_{ad}, θ_{ad}, and φ_{ad} are the polar coordinates associated with the vector from a to the molecular dipole. μ_0 is the molecular dipole moment and, finally, $P_l^m(u)$ are the associated Legendre polynomials.[23]

[1] *Surface Enhanced Raman Scattering,* edited by R. K. Chang and T. E. Furtak (Plenum, New York, 1981).

[2] (a) J. I. Gersten and A. Nitzan, J. Chem. Phys. **75,** 1139 (1981); (b) A. Niztan and L. E. Brus, *ibid.* **75,** 2205 (1981); (c) D. S. Wang and M. Kerker, Phys. Rev. B **25,** 2433 (1982); (d) P. K. Aravind and H. Metiu, Chem. Phys. Lett. **74,** 301 (1980).

[3] (a) A. M. Glass, P. F. Liao, J. G. Bergman, and D. H. Olson, Opt. Lett. **5,** 368 (1980); A. M. Glass, A. Wokaun, J. P. Heritge, J. G. Bergman, P. F. Liao, and O. H. Olson, Phys. Rev. B **24,** 4906 (1981); (b) G. Ritchie and E. Burstein, *ibid.* **24,** 4843 (1981); (c) D. A. Weitz, S. Garoff, C. D. Hanson, T. J. Granila, and J. I. Gersten, J. Lumin. **24/25,** 83 (1981); (d) D. A. Weitz, S. Garoff, J. I. Gersten, and A. Nitzan, J. Chem. Phys. **78,** 5324 (1983).

[4] See Refs. 2(a) and 2(b). For experimental observations of these effects in fluorescence see Ref. 3(d) and also A. Wokaun, H. P. Lutz, A. P. King, U. P. Wild, and R. R. Ernst, J. Chem. Phys. **79,** 509 (1983); For observations of these effects in photochemistry see G. M. Goncher and C. B. Harris, *ibid.* **77,** 3767 (1982); S. Garoff, D. Aa. Weitz, and M. S. Alvarez, Chem. Phys. Lett. **93,** 283 (1982).

[5] For a review see R. R. Chance, A. Prock, and R. Silbey, *Advances in Chemical Physics,* edited by I. Prigogine and S. A. Rice (Wiley, New York, 1978), Vol. 37, p. 1.

[6] P. Avouris and B. N. J. Persson, J. Phys. Chem. **88,** 837 (1984).

[7] H. Metiu, Isr. J. Chem. **22,** 329 (1982).

[8] J. Arias, P. K. Aravind, and H. Metiu, Chem. Phys. Lett. **85,** 404 (1982).

[9] For aggregates of particles, see P. Clippe, R. Evrard, and A. A. Lucas, Phys. Rev. B **14,** 1715 (1976); for surface island films see T. Yamaguchi, S. Yoshida, and A. Kinbara, Thin Solid Films **18,** 63 (1973); **21,** 173 (1974); J. Opt. Soc. Am. **64,** 1563 (1974). For more recent work see Z. Kotler and A. Nitzan, Surf. Sci. **130,** 124 (1983); U. Laor and G. C. Schatz, J. Chem. Phys. **76,** 2888 (1982).

[10] All treatments of the dielectric properties of composites in the Maxwell Garnett approximation also use the same approximation.

[11] J. E. Sansonetti and J. K. Furdyna, Phys. Rev. B **22,** 2866 (1980).

[12] (a) D. J. Bergman, Phys. Rev. B **19,** 2359 (1979); (b) D. J. Bergman, J. Phys. C **12,** 4947 (1979); (c) Y. Kantor and D. Bergman, J. Phys. Chem. **15,** 2033 (1982); (d) J. M. Gerardy and M. Ausloos, Phys. Rev. B **22,** 4950 (1980); **25,** 4204 (1982); (e) For treatments of the two interacting dielectric spheres problem see C. Liang and Y. L. Lo, Radio Sci. **2,** 1481 (1967); S. Levin and G. Olaofe, J. Coll. Interface Sci. **27,** 442 (1968); P. K. Aravind, A. Nitzan, and H. Metiu, Surf. Sci. **110,** 189 (1981); R. Rupin, Phys. Rev. B **26,** 3440 (1982); F. Claro, *ibid.* **25,** 7875 (1982).

[13] M. Inoue and K. Ohtaka, J. Phys. Soc. Jpn. **52,** 3853 (1983).

[14] See Ref. 12(a), D. J. Bergmann, *Lecture Notes in Physics,* edited by R. Burridge, S. Childress, and G. Papanicolaou (Springer, Berlin, 1982), Vol. 154, p. 10.

[15] D. J. Bergman and D. Stroud, Phys. Rev. B **22,** 3527 (1980).

[16] The simplest way to derive Eq. (35) is to take the dipole as a charge q with mass m bound to a center by a harmonic force constant k. Then $\omega = \sqrt{k/m}$ and $\alpha_0 = q^2/(m\omega_0^2)$. When the charge oscillates with amplitude x_0 [e.g., $x(t) = x_0 \cos \omega t$] the energy is

$$(1/2)m(x^2 + \omega_0^2 x^2).$$

Using $\mu = qx$, $\mu_0 = qx_0$ we get Eq. (35).

[17] P. B. Johnson and R. W. Christry, Phys. Rev. B **6,** 4370 (1972). For the size of silver particles (100 Å radius) used in the present calculations the bulk dielectric function of Ag is believed to be suitable. For much smaller particles this dielectric function may be corrected to take into account electron-wall collisions using sandard approximate methods.

[18] N. Liver, J. Jortner, and A. Nitzan (unpublished results).

[19] E. V. Albano, S. Daiser, G. Ertl, R. Miranda, K. Wandelt, and N. Garcia, Phys. Rev. Lett. **51,** 2314 (1983); H. Seki and T. J. Chuang, Chem. Phys. Lett. **100,** 393 (1983).

[20] N. Liver, A. Nitzan, and J. I. Gersten, Chem. Phys. Lett. (in press).

[21] J. D. Jackson, *Classical Electrodynamics,* 2nd ed. (Wiley, New York, 1975), Chap. 4.

[22] M. Danos and L. C. Maximon, J. Math. Phys. **6,** 766 (1965). Application of the general results of this paper to evaluating integrals of the kind [Eqs. (A1) and (A2)] is described in Ref. 14.

[23] Reference 12(a) contains a typographical error [$(-1)^{l'+m'}$ should be $(-1)^{l'+m}$] which is corrected in Eq. (A10).